CSIRO PUBLISHING

COLLECTION | RESEARCH PAPER
https://doi.org/10.1071/WF24205

International Journal of WILDLAND FIRE

International Association of Wildland Fire

Coupling duff development with tree litter and downed fuel inputs, decomposition and fire consumption in a long-term prescribed fire experiment in Florida

Nuria Sánchez-López[A,B,*], Andrew T. Hudak[A], Mac A. Callaham Jr.[C], Melanie K. Taylor[C,D], Toni Viskari[E], Benjamin C. Bright[A], Seth Bigelow[F], Susan Prichard[G], E. Louise Loudermilk[C], Luigi Boschetti[H], Christie Hawley[C] and Deborah Nemens[G]

For full list of author affiliations and declarations see end of paper

***Correspondence to:**
Nuria Sánchez-López
Institute of Natural Resources and Spatial Planning (INDUROT), University of Oviedo, 33600, Mieres, Asturias, Spain
Email: sanchezlnuria.fuo@uniovi.es

Received: 29 November 2024
Accepted: 2 December 2025
Published: 5 February 2026

Cite this: Sánchez-López N *et al.* (2026) Coupling duff development with tree litter and downed fuel inputs, decomposition and fire consumption in a long-term prescribed fire experiment in Florida. *International Journal of Wildland Fire* **35**, WF24205. doi:10.1071/WF24205

ABSTRACT

Background. Mapping surface and ground fuels is key to predicting fire behavior and effects. Remote sensing effectively describes tree canopy attributes, but it is less effective for surface and ground fuels because they are partially obscured by vegetation. **Aims.** We mapped duff loads by leveraging the coupled relationship between canopy, surface and ground fuels: canopy fuels provide the source material for surface fuels, which serve as the material for duff formation. **Methods.** We mapped annual surface fuel production from tree components that contribute to duff formation using airborne laser scanning data. We adjusted a forest soil organic carbon model to simulate duff development under environmental factors constraining decomposition, and included consumption rates accounting for prescribed burning fuel removal. We tested the workflow in southeastern US pine flatwoods where a long-term prescribed burning experiment has been running since 1958. **Key results.** Comparison between modeled duff estimates and field observations provided good agreement, showing low bias and high coefficient of determination. **Conclusions.** This approach allows surface and ground fuels mapping at high spatial resolution (≤5 m) using airborne laser scanning. **Implications.** This integrated modeling workflow improves on current methods to describe heterogeneous duff layers and shows that surface and ground fuels can be mapped using remote sensing and ecological modeling.

Keywords: airborne laser scanning (ALS), annual fuel production, duff, surface fuels, fire return interval (FRI), Florida, organic horizons, prescribed burning, tree biomass, Yasso20, fuel decomposition.

Introduction

Maps of wildland surface fuels (e.g. tree litter, downed woody debris, DWD) and ground fuels (i.e. duff) are needed to support fuel management and predict fire behavior and effects, fuel consumption and atmospheric emissions during fires. Such maps are also key in forest ecosystem analysis, to improve total carbon estimates and the assessment of terrestrial carbon fluxes. Unfortunately, this information is scarce owing to the intrinsic complexity of surface fuels on the forest floor (Keane 2015) and the impracticality of current techniques to capture their spatial variability. Laser scanning systems can capture three-dimensional forest canopy structure at high spatial resolution (Andersen *et al.* 2005; Newnham *et al.* 2015; Wulder *et al.* 2012; Solberg *et al.* 2006; Coops *et al.* 2007; Silva *et al.* 2016; Rocha *et al.* 2023) but have diminishing sensitivity with increased canopy depth, especially to the first 10 cm of the forest floor layer, where

Collection: Multi-scale measurements in support of improved fire, fuel, and smoke models of landscape-level wildland fires most of the dead surface fuel accumulates (Arkin *et al.* 2023; Cova *et al.* 2023; Bright *et al.* 2025). Further, there is a lack of field reference data that reflect the large spatial variability of forest floor conditions. All of this hinders the development of empirical models that are broadly applicable across forested sites.

Maps of surface and ground fuels are particularly relevant in forest ecosystems under frequent prescribed (Rx) fire management, such as longleaf pine (*Pinus palustris* Mill.) flatwoods of the southeastern US. Pine flatwoods are the most extensive terrestrial ecosystem in Florida, but other frequently burned ecosystems in this state include ultraxeric sandhills, upland or high pine, and pine savannas (Varner *et al.* 2003; Boring *et al.* 2017). Pine flatwoods are distinguished from savannas by the marked abundance of shrubs such as saw palmetto (*Serenoa repens* [W. Bartram] Small) and gallberry (*Ilex glabra* [L.] Gray) in the understory. Although detailed fire history studies are lacking, historic fire return interval (FRI) in flatwoods is believed to have been as short as 1–2 years in the past (Harper 1921). This short FRI contributes to vegetation structure that is characterized by the widely sparse arrangement of trees that, in turn, drives the distribution and composition of the dead fine surface fuels (<0.6 mm diameter) on the forest floor, which are dominated by pine needle cast (Prichard *et al.* 2024).

Litter, DWD and duff together are major components of surface and ground fuel beds. In longleaf pine flatwoods, pines are the main tree litter input to the system, which is the focus of this study. Litter (Oi horizon in USDA Soil Taxonomy) is the uppermost layer and is composed of leaves (e.g. needles from pines) and other fine detritus such as cone bracts, flowers, buds, or bark tissue. DWD comprises woody material such as twigs and branches of different sizes. Beneath the litter (Oi horizon) is the duff (composed of both Oe and Oa horizons). Thus, duff is composed of the partially to highly decomposed organic material in the forest floor (Varner *et al.* 2005). In the absence of disturbance, some models have proposed that litterfall and decomposition balance around a 'certain' steady state (Olson 1963; McCaw *et al.* 2002; Zazali *et al.* 2020). Litter decomposition is driven by litter quality, climate and decomposer organisms, resulting in carbon dioxide emissions and duff formation (Prescott 2002; Fierer *et al.* 2005; Keane 2008; Krishna and Mohan 2017; Prescott and Vesterdal 2021). Rx fire management constrains the development of deep duff horizons in forests where fire is frequent owing to consistent low-intensity burning (Varner *et al.* 2005; Mugnani *et al.* 2019; Sánchez-López *et al.* 2025). But when fire is excluded, these forests accumulate deeper duff layers, especially near tree stems where more plant material sloughs off from the trees (Sánchez-López *et al.* 2025). Therefore, forest floor fuel development is intrinsically coupled to vegetation structure and composition as mediated by soils, climate, fire and other disturbances.

Remote sensing can capture inherently heterogeneous vegetation patterns to inform spatially explicit estimation of forest floor fuel distributions. Models can simulate processes of litter and duff accumulation based on vegetation productivity and decomposition rates. Disturbance regimes can be captured spatially (e.g. fire history maps) or expressed as rates (e.g. FRI). A framework that links these complementary information sources provides a promising avenue to help resolve the challenge of mapping these fuels, especially in forested ecosystems where trees dominate biomass production. For effective spatially explicit implementation at nested scales, in previous research, we proposed an integrated modeling approach that predicted individual tree foliage biomass from airborne laser scanning (ALS) data in forests of the southeastern US dominated by longleaf pine (Sánchez-López *et al.* 2023). Annual litter deposition (or litterfall) was calculated as the quotient of foliage biomass over the expected leaf longevity of the dominant species of the study sites. Litter accumulation over time was then determined based on time since fire, applying Olson's accumulation model based on a negative exponential equation (Olson 1963). The accuracy of the estimates was assessed by comparing field data from several locations in the southeastern US, including several flatwoods systems, showing the robustness and transferability of the model.

Process-based biogeochemical soil organic carbon models, such as the Yasso model (Liski *et al.* 2005), have potential use in linking fluxes of canopy materials to duff development. The latest version, Yasso20 (Viskari *et al.* 2022), assumes that forest floor material (i.e. litter, DWD, roots and stumps) are inputs for the development of the humus layer through decomposition (Liski *et al.* 2005; Tuomi *et al.* 2008, 2009, 2011*a*, 2011*b*). Decomposition rates depend on temperature and precipitation inputs to the model and the rates are adjusted according to the size of the decomposing materials, so, for instance, small twigs decay faster than larger branches. Given this model configuration, Yasso20 could be suitable for modeling the accumulation of litter, DWD and duff on the forest floor, especially if inputs of litterfall and DWD annual branchfall are available. A recent study that coupled multitemporal ALS and field information to estimate aboveground biomass implemented Yasso to assess changes in soil carbon (Strîmbu *et al.* 2023). Nevertheless, spatially explicit implementation of this model to characterize surface and/or ground fuels in a frequent-fire ecosystem represents a novel application that invokes fire as an additional ecosystem process that needs to be considered when accounting for the accumulation and removal of fuels on the forest floor.

In this study, we build on the methodology of Sánchez-López *et al.* (2023) to map the aboveground and belowground tree biomass annual contribution to duff formation in a fire-maintained longleaf pine flatwood in Florida (Fig. 1). Sánchez-López *et al.* (2025) recently analyzed patterns of litter and duff accumulation from field records at this same study site, suggesting that Rx burning was a major driver of stand-level accumulation, and aboveground

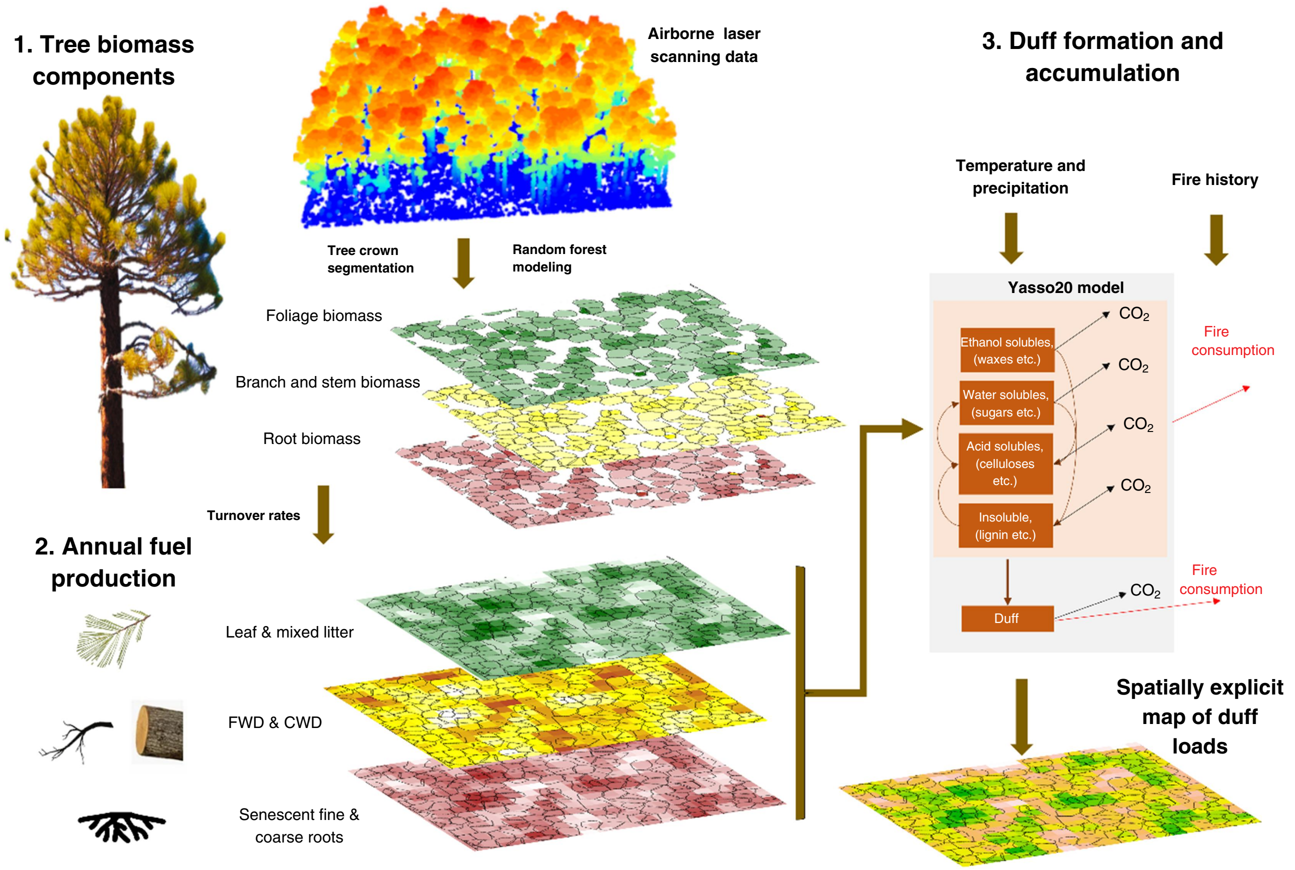

Fig. 1. Workflow to map duff formation and accumulated duff loads in fire-maintained longleaf pine flatwoods of the southeastern US. Airborne laser scanning (ALS) data are used to map tree biomass components. Mass flows annually from the tree components to the surface (fine and coarse downed woody debris – FWD and CWD – and litter) and to the duff layer. We account for decomposition and mass flow between the biomass components and to the duff layer with Yasso20 (architecture adjusted from: https://en.ilmatieteenlaitos.fi/yasso-description). Biomass removal from the system happens through decomposition (respiration, considered by Yasso20) and fuel consumption during prescribed burns (considered in this study).

tree biomass drove the intra-stand distribution of fuels. Therefore, we hypothesized that, in these systems, duff accumulation on the forest floor layer could be explained by spatially explicit tree canopy fuel inputs, climate and Rx fire activity. We first mapped foliage, branch and bole tree biomass using ALS data (Rocha *et al.* 2023; Sánchez-López *et al.* 2023). We used these canopy components to map the aboveground and belowground annual biomass contribution to duff formation and then quantified surface and ground fuel accumulation year by year using Yasso20. The study site hosts a long-term FRI experiment that has produced more than six decades of fire records. Year-by-year fuel accumulation was adjusted based on the Rx fire activity by defining a fuel consumption rate for each fuel bed component. Our first objective was to model duff development in a spatially explicit manner, by coupling surface and ground fuel loads to overstory canopy structure, because the latter is so much more easily, precisely and broadly characterized using remotely sensed data than the former. The second objective was to provide quantitative assessment of the methodology, so we further compared our estimates with field observations (Prichard *et al.* 2024; Callaham *et al.* 2025; Loudermilk *et al.* 2025; Sánchez-López *et al.* 2025).

Materials

Study area

The Osceola National Forest (ONF) study site in northeast Florida (Fig. 2) consists of winter experimental burn units within pine flatwoods communities that are part of a long-term fire experiment established in 1958 in a randomized block design to evaluate the effect of FRI on fuel accumulation. The sites are characterized by low, flat topography situated on poorly drained, acidic sandy soil sometimes underlain by an organic horizon in the mineral soil, which refers loosely to the soil order known as Spodosols (Abrahamson and Hartnett 1990).

The ONF long-term Rx fire experiment comprised six replicates of four treatment units (~0.85 ha each) burned

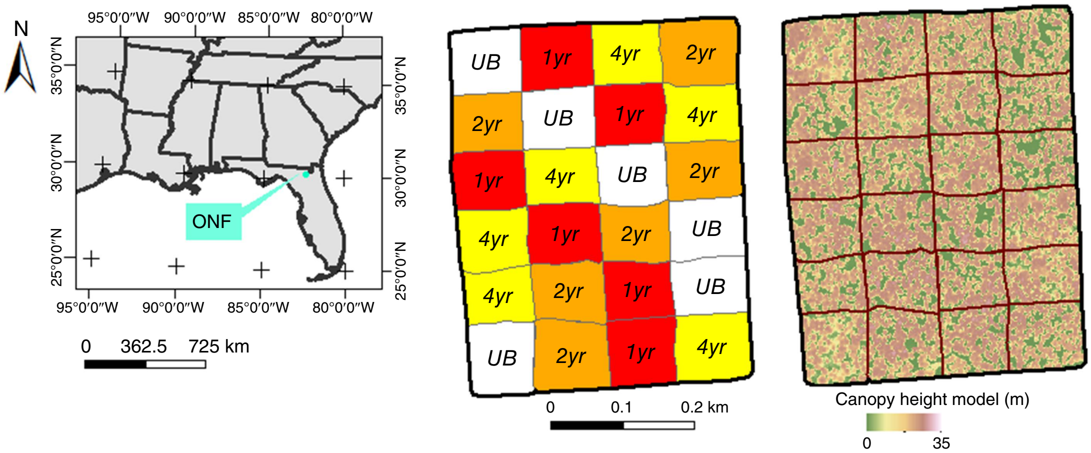

Fig. 2. Location of the Osceola National Forest study site in the southeastern US (left), fire return interval of each burn unit (center), and canopy height model (1 m) derived from airborne laser scanning data. The management units have been burned either every 1, 2, or 4 years or are unburned (UB) since 1958.

at FRIs of 1, 2, or 4 years or not at all (unburned control; McKee 1982). Overstory and understory vegetation was dominated by longleaf pine and saw palmetto respectively. The stand was ~45 years old at the beginning of the experiment in 1958, and it was likely naturally regenerated from a few unmerchantable trees that were left standing after an earlier harvest (D. Wale, unpubl. notes). The treatments have been burned regularly based on the defined FRI with some occasional exceptions that are considered negligible, so we consider the fuel conditions in the research units to be representative of their respective FRI (Fig. 2).

ALS data and tree crown segmentation

Airborne laser scanning data were collected in 2019 and used to map tree crowns and tree biomass components (Rocha *et al.* 2023; Sánchez-López *et al.* 2023). The ALS point cloud was first height-normalized using *LAStools* (Isenburg 2021), and a 1-m resolution canopy height model (Fig. 2) was obtained using the *lidR* R package (Roussel *et al.* 2020). Tree tops were detected and delineated with a segmentation algorithm, and statistics summarizing the point cloud, to be used as predictor variables, were calculated for each tree crown (Eysn *et al.* 2015; Silva *et al.* 2016; Rocha *et al.* 2023; Sánchez-López *et al.* 2023).

Climate data

WorldClim average annual precipitation and monthly average temperature gridded maps (~1 km spatial resolution; Fick and Hijmans 2017) were used as climate inputs for Yasso20. The WorldClim version 2 maps were available in the online repository (https://www.worldclim.org/) for global land areas. These are 1-km rasters interpolated from 30-year climate normals derived from weather station data summarized monthly from 1970 to 2000.

Table 1. Minimum, maximum, mean, standard deviation and coefficient of variation of the pre-fire duff loads measured in the field in 2022.

FRI	Min. duff (kg m^{-2})	Max. duff (kg m^{-2})	Mean duff (kg m^{-2})	s.d. (kg m^{-2})	Coeff. variation (%)
1 year	0.66	9.54	3.05	1.91	62.6
2 years	0.27	8.30	3.29	1.71	52.2
4 years	1.03	10.52	4.27	1.93	45.3
UB	2.33	22.64	8.89	3.94	44.4

Statistics are reported for the three fire return intervals (FRI) treatments and an unburned (UB) control. The size of each clip plot size was 0.01 m^2 and 54 samples were collected per FRI.

Duff measurements

Duff was sampled in all 24 experimental research units in 2022. Three focal trees per unit were randomly selected and geolocated using a Trimble Geo7x GPS (global positioning system). The duff layer was collected in its entirety (i.e. from the bottom of the litter layer to the top of the underlying mineral soil) with a 10 × 10 cm stainless steel duff sampling tool on the north transect 1, 2 and 4 m from the bole of each focal tree (Table 1). Samples were then transported to the laboratory where they were oven dried at 65°C and weighed. Data were collected immediately preceding the Rx fires that took place in February 2022, i.e. 64 years after the experiment started (Callaham *et al.* 2025; Sánchez-López *et al.* 2025).

Methods

We modeled the contribution of tree-derived fuel material to duff formation at annual time steps for 64 years (i.e. from

1958 to 2022) using Yasso20 (Viskari *et al.* 2022), incorporating fire as a surface fuel removal mechanism in addition to decomposition and respiration. Annual, spatially explicit estimates of fuels originating from trees were used as inputs for modeling duff formation. We considered six biomass pools: tree leaf litter, other mixed litter material, fine downed woody debris (FWD, ≤7.6 cm diameter), coarse downed woody debris (CWD, >7.6 cm diameter), and fine and coarse root senescent material (Fig. 1).

Annual fuel production

We first mapped tree foliage, branch, bole and root biomass. Following carbon modeling approaches, turnover rates (Table 2) were then applied to represent annual production, accounting for the expected mortality and senescence that drive the carbon transfer from these pools (White *et al.* 2000; Kurz *et al.* 2009).

Litter annual production

Maps of leaf litter production at 5 m spatial resolution were obtained from previous research that included this same study location. Sánchez-López *et al.* (2023) mapped crown foliage biomass and derived estimates of tree leaf litter production and litter accumulation with time since fire using ALS data to delineate tree crowns in several locations in the southeastern United States. The methodology involved delineating individual tree crowns and computing metrics from the ALS dataset that summarized the point cloud (e.g. maximum height, crown radius, crown length). Tree inventory data from co-located areas were used to estimate foliage biomass based on allometric equations. The individual trees inventoried in the field were linked to the individual tree crowns and a random forest model (Breiman 2001) was trained to predict foliage biomass from crown attributes. A total of 404 observations were used to train the model. The proportion of variance explained by the model was 57.7% and six crown metrics (crown radius, crown base height, the 25th percentile of crown height, crown height variance, crown density and crown length) were the predictors of the model. Additional tree inventory data were used to assess plot-level accuracy of the estimates. For the ONF site, estimates of foliage biomass from the random forest model aggregated at the plot level (8 m radius) compared with estimates of foliage biomass from tree inventory data and allometries (Callaham *et al.* 2025) showed root mean square difference (RMSD) and bias of 0.20 and -0.01 kg m^{-2} respectively.

Vector layers representing the crown loading were rasterized at a spatial resolution of 0.5 m and subsequently resampled to 5-m resolution. Next, a leaf turnover rate, representing the proportion of needles that annually senesce, was used to estimate litterfall (Table 2). Dispersion was modeled using a convolution filter (Sánchez-López *et al.* 2023).

The fine litter pool that contributes to duff formation is composed of categories other than leaf and needle cast. We used data collected at the site (Supplementary Appendix S1) to develop a linear model and predict mixed litter production from pine needle load to represent additional litter components such as fine particles, bark tissue or cones, among others (Supplementary Appendix S2). As considered, this category could include litter inputs from sources other than trees (e.g. shrubs).

Downed woody debris annual production

We predicted and mapped standing crown branch and bole biomass and used these maps as the source of fine and coarse woody material to the forest floor. Both branch and bole biomass were predicted at the tree crown level using random forest modeling, following the approach used for foliage biomass (Breiman 2001; Rocha *et al.* 2023; Sánchez-López *et al.* 2023; Sánchez-López N, Hudak AT, Xia J, *et al.*, unpubl. data). The models reported a proportion of variance explained of 56.3% for branch biomass and 82.0% for the bole biomass. A total of 440 observations were used to train these random forest models. Seven metrics were used as predictors in the branch biomass model (crown radius, crown base height, the 25th percentile of crown height, crown height variance, crown length, crown density and crown spread ratio) and five metrics were retained in the bole biomass model (crown radius, crown base height, the 25th percentile of crown height, crown height variance and crown length). Comparison between aggregated plot-level estimates of tree wood biomass (branch and bole biomass) and plot-level estimates derived from allometries and tree inventory data (Callaham *et al.* 2025) resulted in RMSD

Table 2. Tree biomass pools contributing to duff formation, and turnover biomass rates used to estimate annual production from the corresponding component.

Input biomass pools to duff formation	Tree biomass component	Turnover rate (year^{-1})	Reference
Needles, leaves	Foliage biomass	0.45	Schoettle and Fahey (1994), Holder (2000), White *et al.* (2000), Sánchez-López *et al.* (2023)
Fine branches (<7.6 cm)	Branch biomass	0.035	Kurz (1992), Kurz *et al.* (2009)
Coarse branches and logs (≥7.6 cm)	Stem biomass	0.0045	Kurz (1992), Kurz *et al.* (2009)
Senescent fine roots	Root biomass	0.641	Li *et al.* (2003)
Senescent coarse roots		0.02	Kurz (1992), Kurz *et al.* (1996)

Mixed litter is not included because it is calculated as a function of leaf litter.

and bias of 6.88 and -3.82 kg m^{-2} respectively (Sánchez-López N, Hudak AT, Xia J, *et al.*, unpubl. data).

Values of branch and bole biomass from the tree segmentation were also rasterized at 5-m spatial resolution, and biomass turnover rates from literature were applied to derive annual production estimates of FWD and CWD (Kurz 1992; Kurz *et al.* 2009). We used tree branches as the input for FWD and tree bole biomass as the input for CWD (Table 2). To simulate dispersion of branches from the tree, a convolution filter with a 3 × 3 kernel size was also applied to the 5-m rasterized map (Sánchez-López *et al.* 2023).

Root annual production

Senescent belowground biomass (i.e. root litter) also contributes to duff formation, and the presence of roots in well-developed duff layers has frequently been noted in eastern forests (O'Brien *et al.* 2010; Lajtha *et al.* 2014). Some studies have related biomass dynamics belowground to aboveground, and empirical relationships have been developed from independent data (Li *et al.* 2003; Kurz *et al.* 2009; Reich *et al.* 2014). Drawing from these studies, we estimated the total aboveground tree biomass as the sum of the estimates of foliage, branch and bole biomasses for each tree. Subsequently, we assumed root biomass to be a constant fraction (19.2%) of the aboveground tree biomass (Reich *et al.* 2014). This value represented the average fraction of root biomass of gymnosperms that matches the one reported by Li *et al.* (2003) at 22.2%. The root biomass was partitioned into coarse and fine components using a negative exponential function, following the general formulation by Li *et al.* (2003),

$$\mathrm{Pf} = 0.0072 + 0.357{*}e^{-0.060\mathrm{RB}} \quad (1)$$

where Pf is the fraction of fine root biomass over the total root biomass and RB is the total root biomass. These parameters set yielded an average fraction of ~30%, higher than that obtained using the original equation of Li *et al.*, and were intended to account for additional belowground root biomass associated with the understory vegetation. Biomass turnover rates from literature were then applied to derive root annual production (Table 2).

Duff formation and accumulation

We ran Yasso20 to simulate surface fuel and duff accumulation using the maps of annual production of the different biomass pools as model inputs. Yasso20 divides forest floor material into five chemical components. Four components – celluloses (A), sugars (W), wax-like compounds (E) and lignin-like compounds (N) – encompass decomposing litter, DWD and roots. The fifth component, humus (H), defines stable soil organic carbon. The first four chemical components decompose to another component or are emitted as CO_2 to the atmosphere, and the humus component is only lost as CO_2 (Fig. 1). The decomposition parameters associated with each chemical component are dependent on annual precipitation (mm) and mean monthly temperature (°C).

The inputs to the model were the maps of annual production of leaf litter, mixed litter, CWD, FWD, and fine and coarse senescent roots. We defined the fractions of each component in Yasso20 (A, W, E, N) for each of these input materials based on values for conifer foliage, litter and dead wood reported in previous studies (Supplementary Appendix S3, Supplementary Table S2) (Liski *et al.* 2005; Viskari *et al.* 2022; Strîmbu *et al.* 2023). We used monthly average temperatures and annual precipitation from WorldClim as climate inputs. These datasets were resampled to match the cell size of the annual production maps to run the model on a per pixel basis, but its coarse resolution effectively applied fairly uniform temperature and precipitation values across the study area. We set the parameters of the model per Viskari *et al.* (2022), based on globally available data from the Canadian Intersite Decomposition Experiment, the American Long Term Intersite Decomposition Experiment and the European Intersite Decomposition Experiment (Berg *et al.* 1991*a*, 1991*b*, 1993; Trofymow 1998; Gholz *et al.* 2000). The exception was the pH parameter that controls the mass flow from the first four chemical components (A, W, E, N) to the humus component (H). As originally defined in Yasso, the humus component solely represents the stable soil organic carbon, whereas the duff layer includes both partially and highly decomposed organic material. Therefore, to use Yasso to estimate duff, based on expert evaluation and trial and error tests, we increased the value of the pH parameter to 0.009 from its default 0.004. For the full set of parameters, see Supplementary Appendix S3, Supplementary Table S3.

The duff load at the beginning of the experiment was uncertain. Historical field records reported an average forest floor biomass density of 1.3 kg m^{-2} in 1958. It was not known whether the authors referred only to the litter pool or also included duff. The 1.3 kg m^{-2} value is close to the average litter load (pine needles + mixed litter) reported for the 4-year FRI in 2022 (Supplementary Table S1). The site was maintained using Rx fire on a 5–6 year interval before the experiment started (Taylor *et al.* 2023), so 1.3 kg m^{-2} (for litter only) appears plausible. We defined the initial duff pool assuming an average mass per area similar to the 4-year FRI observed in 2022, i.e. ~4.3 kg m^{-2} (Table 1). Therefore, we selected this FRI as the closest to the Rx burning interval applied at the site before the beginning of the experiment. We distributed the loads based on the litterfall maps, i.e. assuming that there would be more duff under the trees than in gaps. The initial amount of duff present in each of the six biomass pools was calculated based on the proportion that each pool contributed to the annual fuel production. For instance, if leaf litter represented 22% of total annual production, the same proportion was used to define the initial duff pool for that component.

Once the initial duff pool was defined, we ran Yasso20 for 64 years (i.e. representing the time between 1958 and 2022) for each biomass pool. We further adjusted the model to incorporate fire as a process driving the removal of fuel from the forest floor together with decomposition and respiration as considered in Yasso20. Therefore, if an Rx fire was carried out in a specific year (defined by the FRI), proportional amounts of duff and the surface fuel materials were removed from the carbon pool (Table 3). Duff was not removed during the first four years on the 1-year FRI treatments since the original design of the experiment included a 6-year interval instead of annual burns, which was modified starting in 1963 (Sánchez-López *et al.* 2025). Surface fuel consumption rates for litter and FWD were set after evaluation of pre- and post-fire fuel measurements collected at ONF (Supplementary Appendix S4). Pre- and post-fire duff samples were only available from one dataset (Callaham *et al.* 2025). In this case, comparison of average pre- and post- duff loading indicated an unrealistic negative consumption; therefore, we set a conservative duff consumption rate of 3%. We also set a conservative rate of 5% for CWD as no pre- and post- fire data were available for this study site.

Model assessment

Duff predictions from Yasso20 were evaluated by comparing them with the duff measurements for the same year of the running experiment. We assessed the pixel-level accuracy by comparing the predictions of the duff in 5 × 5 m pixels with the field measurements collected in 2022 (Table 1). Measurements taken for the focal trees 1, 2 and 4 m from the tree bole were averaged to represent the duff accumulated at each location, resulting in 72 25-m^2 estimates (i.e. 18 for each FRI). The predicted duff loads corresponded to the sum of the fifth component (H) of the Yasso20 model of each considered biomass pool after year-by-year simulations for the pixel that spatially matched the location of the field plot center, i.e. the focal tree location.

Table 3. Consumption rates assigned to each fuel component.

Fuel material	Consumption rate (%)
Tree leaf litter	80
Mixed litter	50
FWD	40
CWD	5
Duff	3

We did not account for fine or coarse root fire consumption, which we assumed to be negligible.

We calculated the coefficient of determination as the squared correlation between observed and predicted values:

$$R^2 = \frac{\left[\sum_{i=1}^{n}(Y_i - \bar{Y})(\hat{Y}_i - \bar{\hat{Y}})\right]^2}{\sum_{i=1}^{n}(Y_i - \bar{Y})^2 \sum_{i=1}^{n}(\hat{Y}_i - \bar{\hat{Y}})^2} \quad (2)$$

where n is the number of pixel-level measurements, Y_i is the field observed duff biomass (kg m^{-2}) measured within pixel i, $\hat{Y}_i$ is the duff biomass (kg m^{-2}) predicted in pixel i, $\bar{Y}$ is the mean of the observed values and $\bar{\hat{Y}}$ is the mean of the predicted values.

The precision of the predictions was evaluated by computing the RMSD:

$$\mathrm{RMSD} = \sqrt{\frac{\sum_{i=1}^{n}(\hat{Y}_i - Y_i)^2}{n}} \quad (3)$$

The RMSD can be understood as the average difference between predicted and observed values and carries the same units as the observation; smaller values indicate better model fit.

Additionally, the accuracy of the predictions was evaluated by computing the bias:

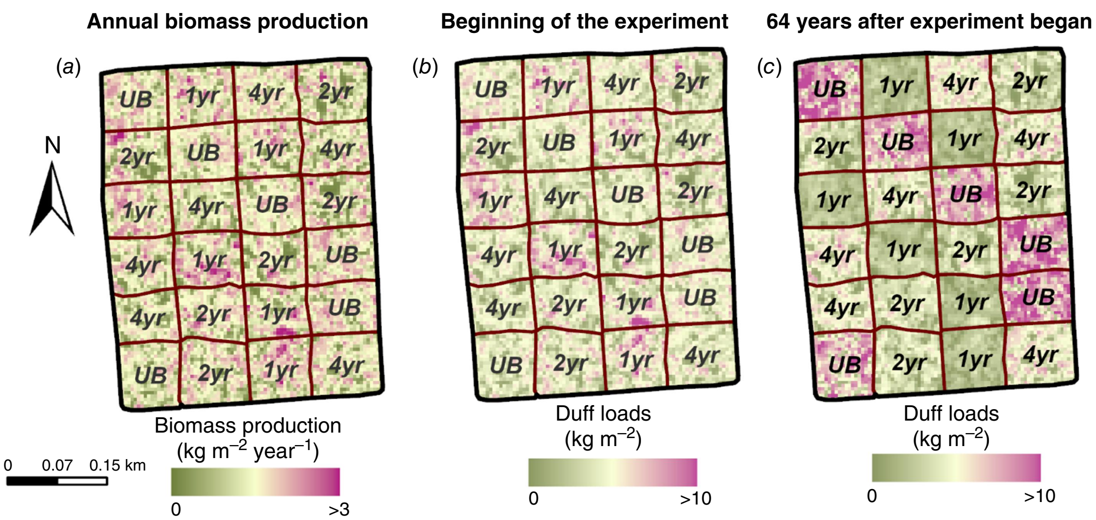

Fig. 3. (*a*) Predicted annual biomass production (including both tree aboveground and belowground components); (*b*) assumed duff loads at the beginning of the study; (*c*) predicted duff loads for the 64th year of the study, consisting of three fire return interval (1, 2, 4 years) treatments and an unburned (UB) control.

$$\text{bias} = \frac{1}{n}\sum_{i=1}^{n}(\hat{Y}_i - Y_i) \quad (4)$$

Accuracy assessment of litter and FWD estimates was also performed if field data were available (Supplementary Appendix S5). Additional historical duff data were also available from 2004. These data were collected within the burn units, but their geolocation was unknown, so we simply compared the average of the duff predictions per burn unit (Supplementary Appendix S6).

Results

Annual fuel production

The combined aboveground and belowground annual production of all the tree components contributing to duff formation was 1.39 kg m^{-2} $year^{-1}$ (Fig. 3*a*). The average annual litter production (i.e. leaf and mixed litter) was 0.59 kg m^{-2} $year^{-1}$, annual DWD production (i.e. FWD and CWD) was 0.14 kg m^{-2} $year^{-1}$ and annual root production (i.e. senescent material from fine and coarse roots) was 0.66 kg m^{-2} $year^{-1}$. Fine roots were the largest contributor to duff formation, accounting for ~44% of the total input material, followed by mixed litter (~23%) and leaf litter (~19%). Aboveground (litter and DWD) and belowground material (roots) contributed 53 and 47% respectively to duff formation (Fig. 4).

Duff formation and accumulation

Average duff loads at the beginning of the experiment and 64 years later were similar (4.30 kg m^{-2} for 1958, and 4.18 kg m^{-2} for 2022). However, there were substantial differences in how duff was distributed across units according to FRIs (Fig. 4*c*, *d*). Our simulations show how duff accumulation changes depending on FRI (Figs 5 and 6).

After 64 years of consistent burning at a specific FRI in each unit, the duff layer reflects different levels of accumulation (Fig. 5), which is also confirmed by field data collected at the study site (Table 1, Callaham *et al.* 2025). The net accumulation of duff depended on the different FRI throughout the 64 years that were covered in this study (Fig. 6). Given the conditions and parameters defined, the 1 and 2-year burned treatments resulted in loss of duff, and the 4-year and unburned treatment resulted in gain of duff although it was negligible in the burn units receiving the 4-year FRI treatment.

Model assessment

Pixel-level RMSD and bias between predicted and observed duff density were 1.93 and −0.05 kg m^{-2}, and the coefficient of determination (R^2) was 0.59 (Fig. 7, Table 4). The model slightly underestimated duff in the 1-year and unburned treatment and overestimated in the 2 and 4-year FRI treatment. Litter and FWD assessments are reported in Supplementary Appendix S5.

Discussion

The goal of this study was to test the feasibility of mapping heterogeneous surface and ground fuel loads by coupling formation and accumulation processes to overstory canopy structure as characterized by ALS data. Maps of surface and ground fuels are required inputs for the new generation of physics-based fire behavior models that will provide more realistic estimates of combustion and emissions during Rx fires (McGrattan *et al.* 2013; Linn *et al.* 2020; Marcozzi *et al.* 2025) and are also key for assessing ecosystem carbon

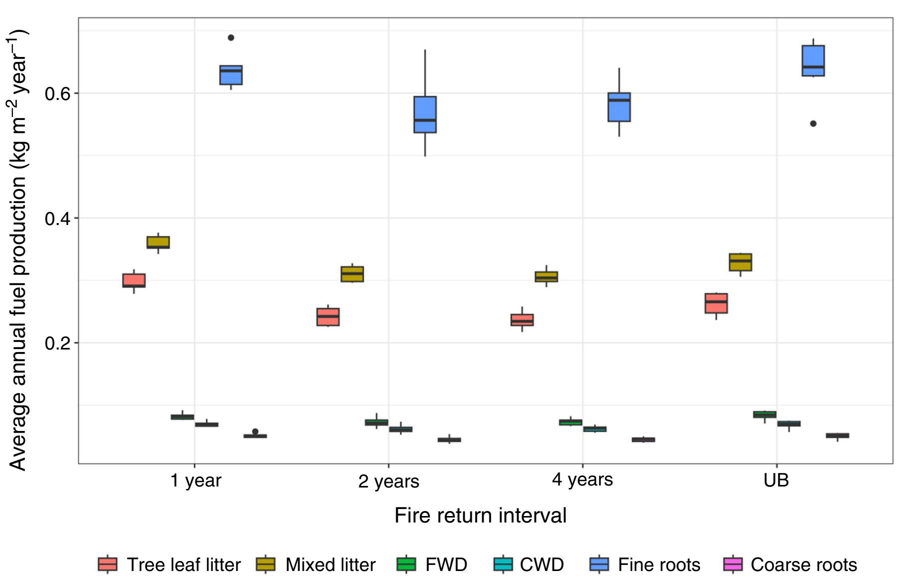

Fig. 4. Boxplots of annual biomass pools contributing to duff formation per fire return interval (FRI). The considered contributing aboveground biomass components are tree leaf litter, mixed litter, fine downed woody debris (FWD), coarse downed woody debris (CWD); the considered contributing tree belowground components are senescent material from fine and coarse roots. Biomass components were estimated from airborne laser scanning data. Boxes represent the interquartile range (25th–75th percentiles) with the median as the central line, and the whiskers extend to the most extreme values within 1.5 times the interquartile range.

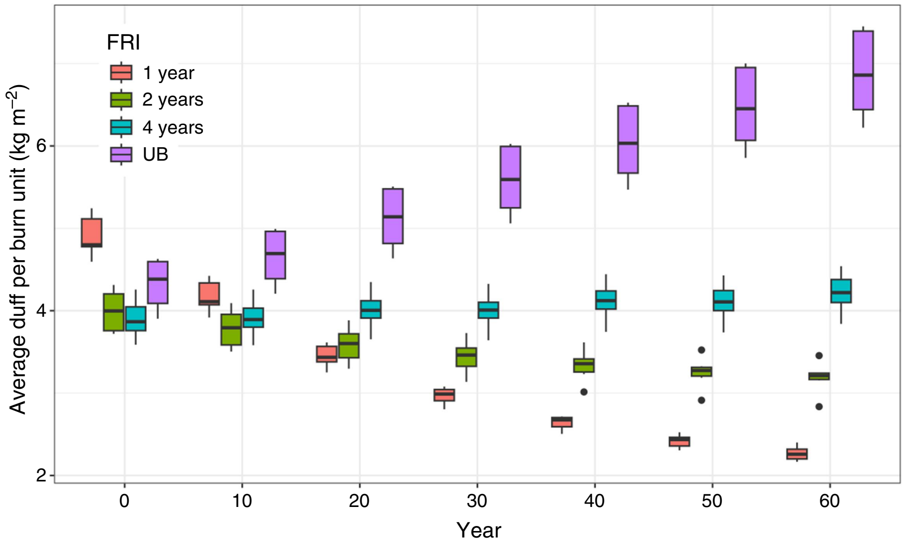

Fig. 5. Boxplots of the modeled duff mass averaged per burn unit and displayed at 10-year intervals in pine flatwoods managed under the three fire return interval (FRIs; 1, 2, 4 years) treatments and an unburned (UB) control. Boxes represent the interquartile range (25th–75th percentiles) with the median as the central line, and the whiskers extend to the most extreme values within 1.5 times the interquartile range.

balance (Li *et al.* 2019). Our modeling approach provided reasonable predictions of specific fuel loads in this long-running study of FRI. Leaf litter in unburned stands was the lone exception in which we greatly overpredicted leaf litter density (Supplementary Appendix S5, Supplementary Fig. S5, Supplementary Table S5). Overall, our approach represents a major advance in the challenging but vital task of describing fuel loads in systems with substantial tree cover.

The accuracy assessment found low negative bias and high correlation of the duff estimates with the field reference dataset (Table 4). The spatial variability of the surface and belowground fuels was constrained to the tree crown maps. The duff reference dataset was collected within 4 m of the tree boles, so it would be expected that duff formation at the sampling locations was mostly driven by the tree litter, DWD and root materials. Although our estimates included mixed litter that may originate from other aboveground components beyond just trees (Supplementary Appendix S2), a negative bias was still expected, especially in the unburned treatments because of the dense understory (mostly saw palmetto) which belowground activity also contributes to duff formation. Although we estimated a higher proportion of fine roots from the aboveground tree biomass to compensate for this effect, belowground inputs may still be underestimated. Most of the saw palmetto leaves burn in the annual and biennial treatments and probably have little influence on fuel accumulation. So, given the 2–2.5 year leaf life span, there is little time for the plant to regrow, senesce and decompose (Hendry and Gholz 1986; Abrahamson 2007). However, the stem or petiole often does not burn, being top-killed and dropping off throughout the year. In the 1-year FRI treatments, the underestimation of duff loads may be driven by the assumption of constant annual duff consumption. In this regard, observations in the field suggest that surface fuel accumulation appears patchier in the 1-year FRI, causing fire to spread unevenly, i.e. creating unburned areas with no fuel consumption and more duff accumulation.

Four major uncertainties remain in our modeling approach: (1) the duff conditions at the beginning of the experiment; (2) the proportion of duff consumed during each Rx burning; (3) the uncertainty of the tree crown fuel and production modeling approaches; and (4) the parameters of Yasso20 controlling duff decomposition and the mass flow from the four chemical components (A, W, E, N) of the forest floor material to the duff. The interaction of these parameters influences predictions of the net duff accumulation. For the first uncertainty, if there were lower duff loads at the beginning of the experiment compared with what we assumed, the mass flow from the forest floor material to duff should have been higher to reach the loads observed on the unburned plots. Similarly, the proportion of duff consumed at each Rx fire would be lower. For the second uncertainty, co-located measurements of duff pre- and post-fire, e.g. by using duff pins, would help to reduce uncertainties in duff consumption (Prichard *et al.* 2017). Available field data included pre- and post-fire duff samples and indicated an implausible negative consumption of duff (Callaham *et al.* 2025; Sánchez-López *et al.* 2025). Sánchez-López *et al.* (2025) conjecture that the sampling protocol was insufficient to characterize the large heterogeneity of duff on the forest floor. For the third uncertainty, the simulations were performed based on estimates of foliage, branch and bole biomass. Overall, these input data showed a good relationship between estimated and observed values. However, reference observations were estimates derived using allometric equations and diameter at breast height of the trees tallied in the field. The use of allometries introduces uncertainties and often better reflects results in local conditions where they were calibrated (Gonzalez-Benecke *et al.* 2014; Samuelson *et al.* 2014). In our case, allometries from southern forest ecosystems were used to minimize this possible influence.

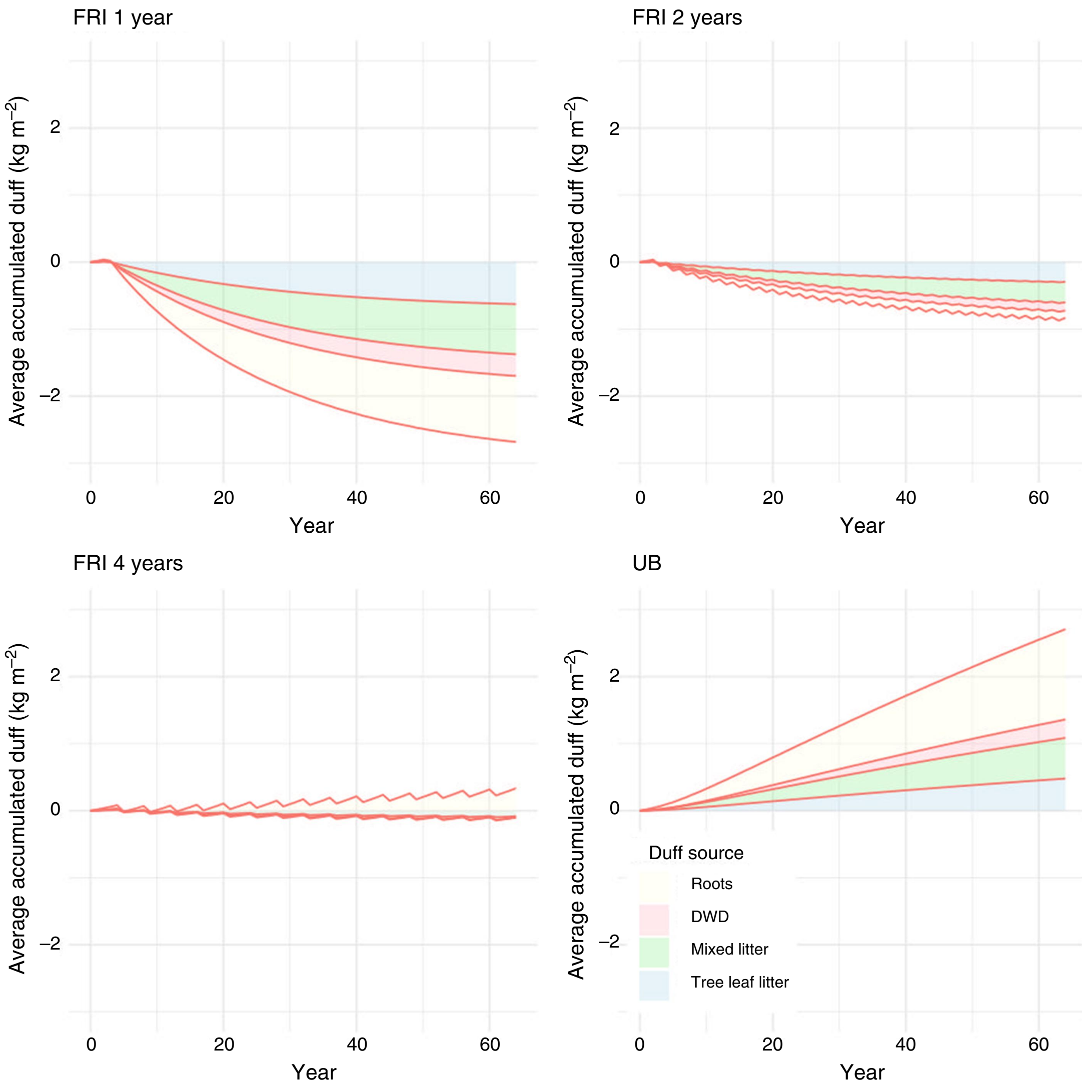

Fig. 6. Average annual variation in duff accumulation based on the considered biomass components contributing to duff formation during 64 years of the long-running study, consisting of three fire return interval (FRIs; 1, 2, 4 years) treatments and an unburned (UB) control. The model predicts duff load from aboveground and belowground biomass inputs, fire frequency and the Yasso20 soil organic carbon model.

However, these uncertainties get propagated when further implementing the ecological-based approach to derive the annual production inputs and the accumulated loads. Patterns of branchfall and litterfall are influenced by annual changes in productivity and episodic disturbance events (e.g. variations in annual precipitation, wind storms). Turnover rates are commonly used in carbon modeling to represent mortality and carbon transfer among pools (White *et al.* 2000; Kurz *et al.* 2009), though we acknowledge this is a simplification, particularly for sporadic events like branchfall and for root turnover because little information is available across ecosystems.

For the fourth uncertainty, our analyses suggest that the global Yasso20 parametrization and/or the assumption that decomposition rates are stable for the different fuel components over time are incorrect. Recent studies have shown that soil organic carbon models with their default parameters could not reliably predict the seasonal and long-term pattern of heterotrophic respiration (Ťupek *et al.* 2019). Additionally, the overestimation of litter in the unburned units (Supplementary Appendix S5, Figs S5 and S6) may be caused by the dataset used to calibrate the decomposition rates, which is based on data collected during several litterbag experiments (Berg *et al.* 1991*a*, 1991*b*; Trofymow 1998; Gholz *et al.* 2000). Overestimation was also observed in Sánchez-López *et al.* (2023), who used annual average actual evapotranspiration (Senay and Kagone 2019) as the predictor of decomposition. That decomposition model was developed using the American Long Term Intersite Decomposition Experiment data (Gholz *et al.* 2000), and these datasets were also used to estimate global parameters for Yasso20

(Viskari *et al.* 2022). These litterbag experiments measured the litter remaining in the bags to determine decomposition. Nevertheless, recent research also suggests that the mass remaining in litter bags could reflect decomposition and accumulation of decomposed material, and a decline in mass loss rate with time would represent the progressive transformation of plant material into slow-cycling microbial decomposition products (Prescott and Vesterdal 2021). Therefore, there may be an underestimation of decomposition that is not accounted for by these methods. Another reason for the discrepancy between modeled and observed duff accumulation rates in the unburned plots may be the shifting composition of the decomposer communities (soil microbes = bacteria and fungi) that occur in the absence of fire. Microbial communities in mineral soils at these same units were significantly different between the unburned and frequently burned treatments (Fox *et al.* 2024), and the unburned soils had a community with greater representation of wood decomposing saprobic fungi. Thus, long-term differences in the amount and type of material available to decomposers appear to select for organisms that have different functional capacities, and this in turn may influence the actual rates of decomposition operating in plots with different fire histories.

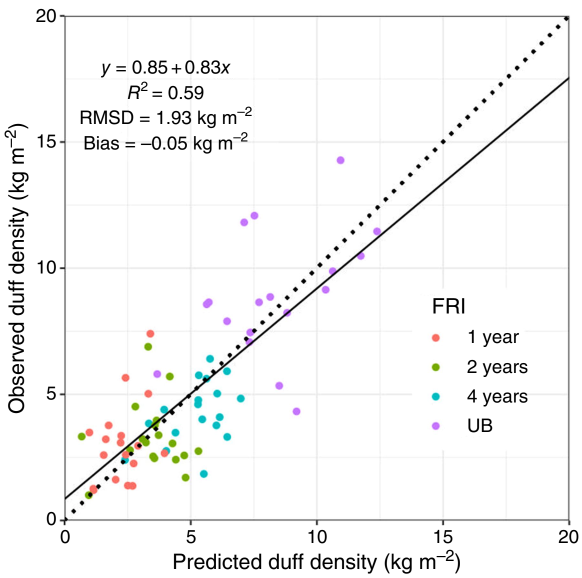

Fig. 7. Goodness of fit (observed vs predicted values) at the pixel-level for the model predicting duff load from aboveground and belowground biomass inputs, fire return interval (FRI) land the Yasso20 soil organic carbon model. The dashed black line represents the 1:1 relationship and the black line represents the linear regression ($y = \beta_0 + \beta_1 x$). UB: unburned treatment.

Our analyses partially neglect the temporal and spatial variability of the surface fuel bed due to tree growth. The simulations were performed given the estimates of foliage and branch biomass based on the most recent ALS dataset available from 2019. Tree crown segmentation was used for the spatial distribution of the annual production litter, DWD and root material. On average, basal area may have changed only slightly during the experiment. Field records reported an average tree diameter of ~28 cm at the beginning of the experiment in 1958 (Ross *et al.* 2024), and the sampling performed in 2022 reported an average of 31.2 cm (Appendix A in Sánchez-López *et al.* 2023). Despite this, it is likely that during the past 64 years, the trees have undergone changes in growth and mortality. Future studies could incorporate growth models (e.g. Forest Vegetation Simulator-FVS; Crookston and Dixon 2005) to further consider these processes on the crown foliage, branch and bole biomass estimates derived from the ALS data, so that both backward and forward predictions in time could align more closely with expected tree growth dynamics.

Prescribed burning (or lack thereof) as a major driver of duff accumulation patterns at ONF and its effects should be carefully addressed when quantifying surface fuel loads. Year-by-year simulations require precise knowledge of the disturbance history of the study site and fire consumption rates, which is especially important for the duff layer. Experimental burns at ONF have been carried out since 1958 and information on the burn dates was available for our analysis. However, the conditions during each burn and the consumption rates are unknown. Field information collected pre- and post-fire provided some guidance on the likely average consumption expected for surface fuels. McKee (1982) also reported a reduction ranging from 33–67% of the weight of the forest floor material under annual or biennial burning.

Table 4. Observed and predicted duff loads at the pixel-level averaged per fire return intervals (FRI), consisting of three FRI treatments (1, 2, 4 years) and an unburned (UB) control; n_p indicates the number of pixel-level measurements; intercept (β_0) and slope (β_1) of the linear regression between the field-based (y) and predicted duff loads (x), coefficient of determination (R^2), root mean square difference (RMSD), and bias.

FRI	n_p	Avg(Y_i) (kg m^{-2})	Avg($\hat{Y}_i$) (kg m^{-2})	β_0	β_1	R^2	RMSD (kg m^{-2})	Bias (kg m^{-2})
1 year	18	3.05	2.28	1.31	0.76	0.15	1.68	-0.77
2 years	18	3.29	3.47	3.07	0.06	0.00	1.73	0.18
4 years	18	4.27	5.25	1.79	0.47	0.20	1.58	0.98
UB	18	8.89	8.29	4.90	0.48	0.19	2.56	-0.60
All	72	4.87	4.82	0.85	0.83	0.59	1.93	-0.05

The McKee report was published 24 years after the experiment started and thus provided some insights on the expected average consumption for these rough treatments, but their sampling likely ignored the duff component, or at least these details were omitted from the report.

Despite some of the simplified modeling assumptions, the model shows good performance to estimate duff loading (Fig. 7, Table 4), which we mostly attribute to introducing duff consumption by prescribed fire in our modeling approach, and quantifying the contribution of major components to duff formation (leaves, DWD and roots). Knowing the fire history allowed us to simulate the disturbance patterns over the six decades of the experiment. The conditions and resulting effects after each fire may vary but, consistently sustained over decades, define the stand-level trends that are reflected in the simulated duff loading. Besides that, we represented the main pools contributing to duff formation. Even if we have under- or overestimated the contribution of specific components, their biases may have offset this, yielding a realistic overall contribution. We captured inter-stand variability better than intra-stand, as shown by the low R^2 of the estimates for the specific FRIs compared with the overall coefficient (Table 4). This suggests that the distribution of duff within each stand may be influenced by other factors that we did not consider and/or, as already pointed out, that the number of field observations within each FRI was not large enough to overcome the highly heterogeneous distribution of duff over the forest floor, because the samples were mostly collected around the tree bole (up to 4 m) (Callaham *et al.* 2025). Duff is highly variable at ONF even under similar climate and disturbance conditions (Sánchez-López *et al.* 2025), which may have large implications in the assessment of carbon sequestration.

Conclusion

This work aims to support managers and fire modelers who require reliable fuels information mapped for decision making before, during and after Rx fires. We tested a modeling workflow that can be used to map surface and ground fuel loads if the fire history is known. Our study advances surface fuel mapping and opens new opportunities for spatially explicit assessment of fire and forest dynamics. Integrated modeling workflows such as this one are a step forward for monitoring ecosystem processes at large scale. There is still a lack of understanding of how the interactions between different ecosystem processes (i.e. net productivity, decomposition, fire behavior) synergistically affect fuel accumulation, especially at operational scales of analysis. Although more research is still needed to address these knowledge gaps, modeling efforts such as this one can inform decision makers tasked to achieve ecosystem management objectives, including maintaining soil health, restoring forest structure, conserving plant biodiversity and reducing fire risk.

Supplementary material

Supplementary material is available online.

References

Abrahamson WG (2007) Leaf traits and leaf life spans of two xeric-adapted palmettos. *American Journal of Botany* **94**, 1297–1308. doi:10.3732/ajb.94.8.1297

Abrahamson WG, Hartnett DC (1990) Pine flatwoods and dry prairies. In 'Ecosystems of Florida'. (Eds RL Myers, JJ Ewel, MH Carr) Available at https://bucknell.elsevierpure.com/en/publications/pine-flatwoods-and-dry-prairies (Ecosystems of Florida. University of Central Florida Press: Orlando) [accessed 2 October 2024]

Andersen H-E, McGaughey RJ, Reutebuch SE (2005) Estimating forest canopy fuel parameters using LIDAR data. *Remote Sensing of Environment* **94**, 441–449. doi:10.1016/j.rse.2004.10.013

Arkin J, Coops NC, Daniels LD, Plowright A (2023) Canopy and surface fuel estimations using RPAS and ground-based point clouds. *Forestry: An International Journal of Forest Research* **98**, 15–28. doi:10.1093/forestry/cpad020

Berg B, Booltink H, Breymeyer A, Ewertsson A, Gallardo A, Holm B, Johansson MB, Koivuoja S, Meentemeyer V, Nyman P (1991a) Data on needle litter decomposition and soil climate as well as site characteristics for some coniferous forest sites. Part I. Site Characteristics. Available at https://agris.fao.org/search/en/providers/122495/records/64775712f2e6fe92b365784f

Berg B, Booltink H, Breymeyer A, Ewertsson A, Gallardo A, Holm B, Johansson MB, Kuovioja S, Meentemeyer V, Nyman P, Olofsson J, Pettersson A-S, Reurslag A, Staaf H, Staaf I, Uba L (1991b) 'Data on needle litter decomposition and soil climate as well as site characteristics for some coniferous forest sites. Part II. Decomposition data.' No. 42. (Swedish University of Agricultural Sciences, Department of Ecology and Environmental Research: Uppsala)

Berg B, Berg MP, Bottner P, Box E, Breymeyer A, De Anta RC, Couteaux M, Escudero A, Gallardo A, Kratz W, Madeira M, Mälkönen E, McClaugherty C, Meentemeyer V, Muñoz F, Piussi P, Remacle J, De Santo AV (1993) Litter mass loss rates in pine forests of Europe and Eastern United States: some relationships with climate and litter quality. *Biogeochemistry* **20**, 127–159. doi:10.1007/BF00000785

Boring LR, Hendricks JJ, Taylor RS, Markewitz D (2017) Ecosystem processes and restoration. In 'Ecological Restoration and Management of Longleaf Pine Forests'. (Eds L Katherine Kirkman, Steven B. Jack) pp. 123–139. (CRC Press: Boca Raton, FL, USA). Available at https://www.taylorfrancis.com/books/edit/10.1201/9781315152141/ecological-restoration-management-longleaf-pine-forests-katherine-kirkman-steven-jack?refId=098cc334-12ab-4522-8e90-8d3734dae836&context=ubx, https://www.taylorfrancis.com/chapters/edit/10.1201/9781315152141-7/ecosystem-processes-restoration-lindsay-boring-joseph-hendricks-scott-taylor-daniel-markewitz

Breiman L (2001) Random forests. *Machine Learning* **45**, 5–32. doi:10.1023/A:1010933404324

Bright BC, Hudak AT, Sánchez-López N, Loudermilk EL, Hawley CM, Rowell E, O'Brien JJ, Flanagan SA, Robertson K, Kato A, Hoffman C, Weise DR, Hiers JK (2025) Comparing biomass consumption estimated from point cloud data versus long-wave infrared imagery during prescribed growing season burns in pine woodlands of the southeastern United States. *International Journal of Wildland Fire* **34**, WF24210. doi:10.1071/WF24210

Callaham MA, Taylor MK, Sánchez-López N, Hudak AT, Bright B (2025) 'Tree inventory and field measurements of litter and duff collected at Osceola National Forest in 2022.' WFSI Data Portal. doi:10.60594/W4XW2V

Coops NC, Hilker T, Wulder MA, St-Onge B, Newnham G, Siggins A, Trofymow JT (2007) Estimating canopy structure of Douglas-fir forest stands from discrete-return LiDAR. *Trees* **21**, 295–310. doi:10.1007/s00468-006-0119-6

Cova GR, Prichard SJ, Rowell E, Drye B, Eagle P, Kennedy MC, Nemens DG (2023) Evaluating close-range photogrammetry for 3D understory fuel characterization and biomass prediction in pine forests. *Remote Sensing* **15**, 4837. doi:10.3390/rs15194837

Crookston NL, Dixon GE (2005) The forest vegetation simulator: a review of its structure, content, and applications. *Computers and Electronics in Agriculture* **49**, 60–80. doi:10.1016/j.compag.2005.02.003
Eysn L, Hollaus M, Lindberg E, Berger F, Monnet J-M, Dalponte M, Kobal M, Pellegrini M, Lingua E, Mongus D (2015) A benchmark of lidar-based single tree detection methods using heterogeneous forest data from the alpine space. *Forests* **6**, 1721–1747. doi:10.3390/f6051721
Fick SE, Hijmans RJ (2017) WorldClim 2: new 1-km spatial resolution climate surfaces for global land areas. *International Journal of Climatology* **37**, 4302–4315. doi:10.1002/joc.5086
Fierer N, Craine JM, McLauchlan K, Schimel JP (2005) Litter quality and the temperature sensitivity of decomposition. *Ecology* **86**, 320–326. doi:10.1890/04-1254
Fox S, Taylor MK, Jumpponen A (2024) Fire-excluded and frequently burned longleaf pine forests have contrasting soil microbial communities *Forest Ecology and Management* **551**, 121519.
Gholz HL, Wedin DA, Smitherman SM, Harmon ME, Parton WJ (2000) Long-term dynamics of pine and hardwood litter in contrasting environments: toward a global model of decomposition. *Global Change Biology* **6**, 751–765. doi:10.1046/j.1365-2486.2000.00349.x
Gonzalez-Benecke CA, Gezan SA, Albaugh TJ, Allen HL, Burkhart HE, Fox TR, Jokela EJ, Maier CA, Martin TA, Rubilar RA (2014) Local and general above-stump biomass functions for loblolly pine and slash pine trees. *Forest Ecology and Management* **334**, 254–276. doi:10.1016/j.foreco.2014.09.002
Harper RM (1921) 'Geography of central Florida.' (Florida Geological Survey: FL, USA)
Hendry LC, Gholz HL (1986) Aboveground phenology in North Florida slash pine plantations. *Forest Science* **32**, 779–788. doi:10.1093/forestscience/32.3.779
Holder CD (2000) Geography of *Pinus elliottii* Engelm. and *Pinus palustris* Mill. leaf life-spans in the southeastern USA. *Journal of Biogeography* **27**, 311–318. doi:10.1046/j.1365-2699.2000.00418.x
Isenburg M (2021) LAStools – efficient LiDAR processing software (version 201124, academic rapidlasso GmbH). Available at https://rapidlasso.com/lastools/
Keane RE (2008) Biophysical controls on surface fuel litterfall and decomposition in the northern Rocky Mountains, USA. *Canadian Journal of Forest Research* **38**, 1431–1445. doi:10.1139/X08-003
Keane RE (2015) 'Wildland fuel fundamentals and applications.' (Springer)
Krishna MP, Mohan M (2017) Litter decomposition in forest ecosystems: a review. *Energy, Ecology and Environment* **2**, 236–249. doi:10.1007/s40974-017-0064-9
Kurz WA (1992) Carbon budget of the Canadian forest sector, Phase I. Information report No.X-326. Available at https://www.osti.gov/etdeweb/biblio/5510586 [accessed 18 September 2025]
Kurz WA, Beukema SJ, Apps MJ (1996) Estimation of root biomass and dynamics for the carbon budget model of the Canadian forest sector. *Canadian Journal of Forest Research* **26**, 1973–1979. doi:10.1139/x26-223
Kurz WA, Dymond CC, White TM, Stinson G, Shaw CH, Rampley GJ, Smyth C, Simpson BN, Neilson ET, Trofymow JA, Metsaranta J, Apps MJ (2009) CBM-CFS3: a model of carbon-dynamics in forestry and land-use change implementing IPCC standards. *Ecological Modelling* **220**, 480–504. doi:10.1016/j.ecolmodel.2008.10.018
Lajtha K, Bowden RD, Nadelhoffer K (2014) Litter and root manipulations provide insights into soil organic matter dynamics and stability. *Soil Science Society of America Journal* **78**, S261–S269. doi:10.2136/sssaj2013.08.0370nafsc
Li S, Yuan W, Ciais P, Viovy N, Ito A, Jia B, Zhu D (2019) Benchmark estimates for aboveground litterfall data derived from ecosystem models. *Environmental Research Letters* **14**, 084020. doi:10.1088/1748-9326/ab2ee4
Li Z, Kurz WA, Apps MJ, Beukema SJ (2003) Belowground biomass dynamics in the Carbon Budget Model of the Canadian Forest Sector: recent improvements and implications for the estimation of NPP and NEP. *Canadian Journal of Forest Research* **33**, 126–136. doi:10.1139/x02-165
Linn RR, Goodrick SL, Brambilla S, Brown MJ, Middleton RS, O'Brien JJ, Hiers JK (2020) QUIC-fire: a fast-running simulation tool for prescribed fire planning. *Environmental Modelling & Software* **125**, 104616. doi:10.1016/j.envsoft.2019.104616
Liski J, Palosuo T, Peltoniemi M, Sievänen R (2005) Carbon and decomposition model Yasso for forest soils. *Ecological Modelling* **189**, 168–182. doi:10.1016/j.ecolmodel.2005.03.005
Loudermilk EL, Hawley C, Payne I, Hoffman C, Hudak A, Pokswinski S (2025) Vegetation Biomass, Voxel, and Macroplot Geographical Location Data collected at the Winter Burn Plots located at Osceola National Forest in December 2021 and February 2022. WFSI Data Portal. doi:10.60594/W4X305
Marcozzi A, Wells L, Parsons R, Mueller E, Linn R, Hiers JK (2025) FastFuels: advancing wildland fire modeling with high-resolution 3D fuel data and data assimilation. *Environmental Modelling & Software* **183**, 106214. doi:10.1016/j.envsoft.2024.106214
McCaw WL, Neal JE, Smith RH (2002) Stand characteristics and fuel accumulation in a sequence of even-aged Karri (*Eucalyptus diversicolor*) stands in south-west Western Australia. *Forest Ecology and Management* **158**, 263–271. doi:10.1016/S0378-1127(00)00719-2
McGrattan K, Hostikka S, McDermott R, Floyd J, Weinschenk C, Overholt K (2013) 'Fire dynamics simulator user's guide'. NIST special publication 1019(6). pp. 1–339.
McKee WH (1982) 'Changes in soil fertility following prescribed burning on coastal plain pine sites.' (US Department of Agriculture, Southeastern Forest Experiment Station)
Mugnani MP, Robertson KM, Miller DL, Platt WJ (2019) Longleaf pine patch dynamics influence ground-layer vegetation in old-growth pine savanna. *Forests* **10**, 389. doi:10.3390/f10050389
Newnham GJ, Armston JD, Calders K, Disney MI, Lovell JL, Schaaf CB, Strahler AH, Danson FM (2015) Terrestrial Laser Scanning for Plot-Scale Forest Measurement. *Current Forestry Reports* **1**, 239–251. doi:10.1007/s40725-015-0025-5
O'Brien JJ, Kevin Hiers J, Mitchell RJ, Varner JM, Mordecai K (2010) Acute physiological stress and mortality following fire in a long-unburned longleaf pine ecosystem. *Fire Ecology* **6**, 1–12. doi:10.4996/fireecology.0602001
Olson JS (1963) Energy storage and the balance of producers and decomposers in ecological systems. *Ecology* **44**, 322–331. doi:10.2307/1932179
Prescott CE (2002) The influence of the forest canopy on nutrient cycling. *Tree Physiology* **22**, 1193–1200. doi:10.1093/treephys/22.15-16.1193
Prescott CE, Vesterdal L (2021) Decomposition and transformations along the continuum from litter to soil organic matter in forest soils. *Forest Ecology and Management* **498**, 119522. doi:10.1016/j.foreco.2021.119522
Prichard SJ, Kennedy MC, Wright CS, Cronan JB, Ottmar RD (2017) Predicting forest floor and woody fuel consumption from prescribed burns in southern and western pine ecosystems of the United States. *Forest Ecology and Management* **405**, 328–338. doi:10.1016/j.foreco.2017.09.025
Prichard SJ, Watts AC, Rowell E, Cronan J, Hudak AT, Parsons RA, Kennedy MC, Loudermilk EL, Skowronski NS, Batchelor J, Cova GR, Bester M, Bright BC, Drye B, Eagle P, Nemens DG, Satterfield L, Thoreson J (2024) '3D Fuels: Hierarchically scaled datasets for three-dimensional wildland fuel characterization'. Final Report to SERDP RC-1064. Available at https://depts.washington.edu/flame/docs/SERDP_RC1064_Final_Report_Aug2024.pdf
Reich PB, Luo Y, Bradford JB, Poorter H, Perry CH, Oleksyn J (2014) Temperature drives global patterns in forest biomass distribution in leaves, stems, and roots. *Proceedings of the National Academy of Sciences* **111**, 13721–13726. doi:10.1073/pnas.1216053111
Rocha KD, Silva CA, Cosenza DN, Mohan M, Klauberg C, Schlickmann MB, Xia J, Leite RV, Almeida DRA de, Atkins JW, Cardil A, Rowell E, Parsons R, Sánchez-López N, Prichard SJ, Hudak AT (2023) Crown-level structure and fuel load characterization from airborne and terrestrial laser scanning in a longleaf pine (*Pinus palustris* Mill.) forest ecosystem. *Remote Sensing* **15**, 1002. doi:10.3390/rs15041002
Ross CW, Loudermilk EL, O'Brien JJ, Flanagan SA, McDaniel J, Aubrey DP, Lowe T, Hiers JK, Skowronski NS (2024) Lidar-derived estimates of forest structure in response to fire frequency. *Fire Ecology* **20**, 44. doi:10.1186/s42408-024-00279-7
Roussel J-R, Auty D, Coops NC, Tompalski P, Goodbody TR, Meador AS, Bourdon J-F, de Boissieu F, Achim A (2020) lidR: an R package for

analysis of Airborne Laser Scanning (ALS) data. *Remote Sensing of Environment* **251**, 112061. doi:10.1016/j.rse.2020.112061

Samuelson LJ, Stokes TA, Butnor JR, Johnsen KH, Gonzalez-Benecke CA, Anderson P, Jackson J, Ferrari L, Martin TA, Cropper WP (2014) Ecosystem carbon stocks in *Pinus palustris* forests. *Canadian Journal of Forest Research* **44**, 476–486. doi:10.1139/cjfr-2013-0446

Sánchez-López N, Hudak AT, Boschetti L, Silva CA, Robertson K, Loudermilk EL, Bright BC, Callaham MA, Taylor MK (2023) A spatially explicit model of tree leaf litter accumulation in fire maintained longleaf pine forests of the southeastern US. *Ecological Modelling* **481**, 110369. doi:10.1016/j.ecolmodel.2023.110369

Sánchez-López N, Hudak AT, Taylor MK, Callaham MA, O´Brien JJ (2025) "Is this duff? Long-term prescribed burning effects in litter and duff in pine flatwoods of the southeastern US." *Fire Ecology* (2025). doi:10.1186/s42408-025-00425-9

Sánchez-López N, Hudak AT, Bright B (2026) Estimated tree biomass, surface and ground fuel annual deposition, and accumulated fuel surface and ground fuel loading in 2022 at the Macon Fire Study, Osceola National Forest. WFSI Data Portal. doi:10.60594/W45C7R

Schoettle AW, Fahey TJ (1994) Foliage and fine root longevity of pines. *Ecological Bulletins* **43**, 136–153.

Senay G, Kagone S (2019) 'Daily SSEBop Evapotranspiration Data from 2000 to 2018.' doi:10.5066/P9L2YMV

Silva CA, Hudak AT, Vierling LA, Loudermilk EL, O'Brien JJ, Hiers JK, Jack SB, Gonzalez-Benecke C, Lee H, Falkowski MJ (2016) Imputation of individual longleaf pine (*Pinus palustris* Mill.) tree attributes from field and LiDAR data. *Canadian Journal of Remote Sensing* **42**, 554–573. doi:10.1080/07038992.2016.1196582

Solberg S, Naesset E, Bollandsas OM (2006) Single tree segmentation using airborne laser scanner data in a structurally heterogeneous spruce forest. *Photogrammetric Engineering & Remote Sensing* **72**, 1369–1378.

Strîmbu VF, Næsset E, Ørka HO, Liski J, Petersson H, Gobakken T (2023) Estimating biomass and soil carbon change at the level of forest stands using repeated forest surveys assisted by airborne laser scanner data. *Carbon Balance and Management* **18**, 10. doi:10.1186/s13021-023-00222-4

Taylor MK, Strother DJ, Callaham MA Jr. (2023) Fire exclusion reduces A-horizon thickness in a long-term prescribed fire experiment in Spodosols of northern Florida, USA. *Soil Science Society of America Journal* **87**, 425–429. doi:10.1002/saj2.20507

Trofymow JA (1998) The Canadian Intersite Decomposition ExperimenT (CIDET): project and site establishment report. No. BC-X-378. 1998.

Tuomi M, Vanhala P, Karhu K, Fritze H, Liski J (2008) Heterotrophic soil respiration—comparison of different models describing its temperature dependence. *Ecological Modelling* **211**, 182–190. doi:10.1016/j.ecolmodel.2007.09.003

Tuomi M, Thum T, Järvinen H, Fronzek S, Berg B, Harmon M, Trofymow JA, Sevanto S, Liski J (2009) Leaf litter decomposition—Estimates of global variability based on Yasso07 model. *Ecological Modelling* **220**, 3362–3371. doi:10.1016/j.ecolmodel.2009.05.016

Tuomi M, Laiho R, Repo A, Liski J (2011*a*) Wood decomposition model for boreal forests. *Ecological Modelling* **222**, 709–718. doi:10.1016/j.ecolmodel.2010.10.025

Tuomi M, Rasinmäki J, Repo A, Vanhala P, Liski J (2011*b*) Soil carbon model Yasso07 graphical user interface. *Environmental Modelling & Software* **26**, 1358–1362. doi:10.1016/j.envsoft.2011.05.009

Ťupek B, Launiainen S, Peltoniemi M, Sievänen R, Perttunen J, Kulmala L, Penttilä T, Lindroos A-J, Hashimoto S, Lehtonen A (2019) Evaluating CENTURY and Yasso soil carbon models for CO_2 emissions and organic carbon stocks of boreal forest soil with Bayesian multi-model inference. *European Journal of Soil Science* **70**, 847–858. doi:10.1111/ejss.12805

Varner JM, Kush JS, Meldahl RS (2003) Structural characteristics of frequently-burned old-growth longleaf pine stands in the mountains of Alabama. *Castanea* **68**, 211–221.

Varner JM, Gordon DR, Putz FE, Hiers JK (2005) Restoring fire to long-unburned *Pinus palustris* ecosystems: novel fire effects and consequences for long-unburned ecosystems. *Restoration Ecology* **13**, 536–544. doi:10.1111/j.1526-100x.2005.00067.x

Viskari T, Pusa J, Fer I, Repo A, Vira J, Liski J (2022) Calibrating the soil organic carbon model Yasso20 with multiple datasets. *Geoscientific Model Development* **15**, 1735–1752. doi:10.5194/gmd-15-1735-2022

White MA, Thornton PE, Running SW, Nemani RR (2000) Parameterization and sensitivity analysis of the BIOME–BGC terrestrial ecosystem model: net primary production controls. *Earth Interactions* **4**, 1–85. doi:10.1175/1087-3562(2000)004<0003:PASAOT>2.0.CO;2

Wulder MA, White JC, Nelson RF, Næsset E, Ørka HO, Coops NC, Hilker T, Bater CW, Gobakken T (2012) Lidar sampling for large-area forest characterization: A review. *Remote Sensing of Environment* **121**, 196–209. doi:10.1016/j.rse.2012.02.001

Zazali HH, Towers IN, Sharples JJ (2020) A critical review of fuel accumulation models used in Australian fire management. *International Journal of Wildland Fire* **30**, 42–56. doi:10.1071/WF20031

Data availability. Tree biomass estimates, annual fuel production estimates, and accumulated surface and ground fuel load estimates by component for the year 2022 derived from the Yasso20 simulations, as described in this publication, are archived for public access in the Wildland Fire Science Initiative (WFSI) data portal in the data product of Sánchez-López *et al*. (2026). The field data used for the accuracy assessment that supports this study are also publicly available in the WIFSI data portal (Callaham *et al*. 2025; Loudermilk *et al*. 2025). The additional field data used in the Appendices for assessment, and that is not currently public, will be made available on request. Worldclim data are available at https://www.worldclim.org/. Airborne laser scanning data corresponding to Baker county (Florida), where the study site is located, are available for downloading from the US Geological Survey (https://www.floridagio.gov/pages/lidar-resources).

Conflicts of interest. Andrew T. Hudak is an Associate Editor of the *International Journal of Wildland Fire* but was not involved in the peer review or decision-making process for this paper. The authors declare no other conflicts of interest.

Declaration of funding. Funding was provided by the DOD Strategic Environmental Research and Development Program (SERDP) award RC20-1346 to the US Forest Service Rocky Mountain Research Station. This research was supported by the USDA Forest Service, Rocky Mountain Research Station and the Southern Research Station. The findings and conclusions in this publication are those of the authors and should not be construed to represent any official USDA or US Government determination or policy.

Acknowledgements. We express our gratitude to the forest managers, personnel and fire practitioners in the Osceola National Forest and Osceola Ranger District, who have maintained the long-term fire treatments in this study site since 1958. We thank all the crews and technicians who contributed to the collection of the field datasets used in this study, and especially Gregg Chapman who was instrumental during the duff field campaign carried out in 2022.

Author contributions. Conceptualization: N. S. L, A. T. H., M. A. C.; methodology: N. S. L., A. T. H.; data curation: N. S. L.; formal analysis: N. S. L.; software: N. S. L., B. C. B., T. V.; validation: N. S. L.; investigation: N. S. L., A. T. H.; resources: N. S. L., A. T. H., M. A. C., M. K. T., E. L. L., C. H., S. P., D. N.; original draft preparation: N. S. L., A. T. H.; writing – review and editing: N. S. L., A. T. H., M. A. C., M. K. T., S. B., S. P., L. B., T. V., B. C. B., E. L. L., C. H.; visualization: N. S. L.; funding acquisition: A. T. H. All authors have read and agreed to the submitted version of the manuscript.

Author affiliations

[A]USDA Forest Service, Rocky Mountain Research Station, Forestry Sciences Laboratory, 1221 S Main Street, Moscow, ID, USA.

[B]Institute of Natural Resources and Spatial Planning (INDUROT), University of Oviedo, Mieres, 33600 Asturias, Spain.

[C]USDA Forest Service, Southern Research Station, Disturbance and Prescribed Fire Laboratory, 320 Green Street, Athens, GA, USA.

[D]North Carolina State University, Center for Geospatial Analytics, 2800 Faucette Drive, Raleigh, NC, USA.

[E]Finnish Meteorological Institute, Helsinki, Finland.

[F]Tall Timbers Research Station & Land Conservancy, 13093 Henry Beadel Drive, Tallahassee, FL, USA.

[G]School of Environmental and Forest Sciences, University of Washington, Seattle, WA 98195, USA.

[H]Department of Forest, Rangeland and Fire Sciences, College of Natural Resources, University of Idaho, Moscow, ID, USA.